

OPTICAL MODEL OF THE NUCLEUS WITH A POLYNOMIAL POTENTIAL

A. V. LUK'YANOV, Yu. V. ORLOV, and V. V. TUROVTSEV

Nuclear Physics Institute, Moscow State University

Submitted to JETP editor June 6, 1961

J. Exptl. Theoret. Phys. (U.S.S.R.) 41, 1634-1643 (November, 1961)

A study is made of the shape of the potential for the nuclear optical model with surface absorption. For a polynomial potential, we choose a set of parameters which gives a good description of the experimental data on scattering of 14 Mev neutrons. A comparison is made of various potentials.

1. INTRODUCTION

EXTENSIVE use is made at present of the optical model with a potential whose real part has the form proposed by Woods and Saxon.^[1] However, as we have shown previously,^[2] from an investigation of a polynomial potential with volume absorption and not including spin-orbit interaction, the polynomial potential leads to similar results, other things being equal. Although the optical model with volume absorption and omitting spin-orbit interaction gives the correct dependence of the integral cross sections (total cross section σ_t , elastic scattering σ_s and absorption σ_r) on mass number A for medium and heavy nuclei and describes the qualitative features of the differential elastic scattering cross section for $\theta < 90^\circ$, it nevertheless has various deficiencies. In the region of light nuclei, the cross section ratio σ_s/σ_r is too high compared with experiment, the computed differential cross sections have deep minima which are not seen experimentally and the backward scattering is too large. The work of Bjorklund and Fernbach^[3] (which we abbreviate as BF) shows that this defect can be eliminated by using a potential which includes spin-orbit interaction and which has a maximum of its imaginary part at the nuclear boundary (surface absorption). In the present work we have investigated the optical model with surface absorption and including effects of spin-orbit interaction, but in contrast to the work of BF, in which the real part was the Woods-Saxon potential and the imaginary part was Gaussian, we describe the potential by means of polynomials.

2. THE POLYNOMIAL POTENTIAL

We have found the parameter values which give agreement with the experimental data on scattering

of 14-Mev neutrons for a nuclear potential of the following form* (cf. Fig. 1):

$$V = V_{CR}\rho(r) + iV_{CI}q(r) - V_{SR}\left(\frac{\hbar}{\mu c}\right)^2 \frac{1}{r} \frac{d\rho}{dr} \sigma_1;$$

$$\rho(r) = \begin{cases} 1, & 0 \leq r \leq R - d_r \\ \frac{1}{2} - \frac{15}{16} \left(\frac{r-R}{d_r}\right) \left[\frac{1}{5} \left(\frac{r-R}{d_r}\right)^4 - \frac{2}{3} \left(\frac{r-R}{d_r}\right)^2 + 1 \right], & R - d_r \leq r \leq R + d_r \\ 0, & r \geq R + d_r \end{cases} \quad (1)$$

$$q(r) = \begin{cases} 0, & 0 \leq r \leq R - d_i \\ \left[1 - \left(\frac{r-R}{d_i}\right)^2 \right]^2, & R - d_i \leq r \leq R + d_i \\ 0, & r \geq R + d_i \end{cases}$$

where $R = (r_0 A^{1/3} + \delta)$ and μ is the π -meson rest mass.

The determination of the phases and cross sections was done by standard methods, by a numerical solution of the Schrödinger equation with the potential (1) in the region $R - d \leq r \leq R + d$, where $d = \max\{d_r, d_i\}$. The method was essentially the same as that described previously.^[2] The pair of second-order differential equations corresponding to the two directions of the neutron spin was reduced to a system of first-order equations, which was solved by the Runge-Kutta method. As initial conditions we chose the function and its first derivative at the point $r = R - d$, where their analytic expressions are known.

It is a very difficult problem to vary simultaneously all the parameters of the potential (V_{CR} , V_{CI} , V_{SR} , d_r , d_i , r_0 and δ). However the solution is simplified by the fact that the range of parameter

*After this work was completed, there appeared the paper of Green et al.^[4] on a nonlocal optical model, in which the real part of the potential is also described by a fifth-degree polynomial.

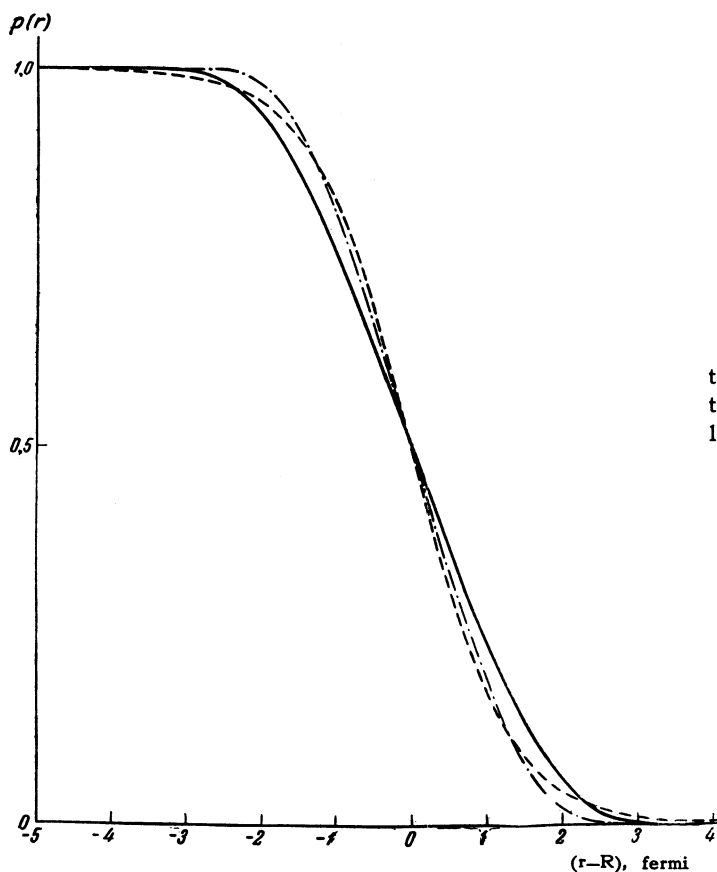


FIG. 1. Real parts of the potentials. Solid curve—potential (1) with the parameters of (3); dashed curve—potential (4); dot-dashed curve— for potential (1) giving least squares fit to potential (4).

values and the behavior of the cross section as a function of certain of them has been studied fairly well. In particular this enables us beforehand to make a reasonable choice of the parameters V_{CR} and V_{SR} . Fixing V_{CR} subject to the condition that the parameters r_0 and δ , which determine the nuclear radius, remain free, is entirely permissible because of the well known ambiguity of the type $V_{CR}-R$. Thus the value $V_{CR} = 44$ Mev is definitely acceptable, since it surely lies in the right range (it coincides with the value used in [3]). The value $V_{SR} = 7.7$ Mev was taken from the work of Levintov. [6] Changing this parameter within reasonable limits has an insignificant effect on the cross sections (in particular on the integral cross sections). It might be improved by using data on the polarization of scattered neutrons, but unfortunately there are as yet no such data for 14 Mev neutrons.

In choosing the other parameters, we used computations showing the variation of the cross section when each of the parameters d_r , d_i and V_{CI} was changed individually. Over a wide range of values, the dependence of the cross sections σ_t and σ_r on the parameters d_r and d_i is close to linear, which greatly simplifies the problem of choosing these parameters. To good accuracy, the cross sections σ_t and σ_r , as functions of d_r with all other parameters fixed, can be represented as

$$\sigma = \sigma^{(0)} + \alpha d_r. \quad (2)$$

The value of $\sigma^{(0)}$ is independent of d_r ; the coefficient α is almost constant for medium and heavy nuclei ($\alpha \sim 33$ fermi for σ_r , $\alpha \sim 40$ fermi for σ_t), and is somewhat lower for the light nuclei ($\alpha \sim 15$ fermi for σ_r , $\alpha \sim 30$ fermi for σ_t). The closeness of the values of α for σ_t and σ_r in the first case indicates a weaker dependence of the integral elastic scattering on the parameter d_r . But the shape of the angular distribution of the elastically scattered neutrons is extremely sensitive to changes of the parameter d_r . With increasing d_r , the oscillations in the diffraction pattern become less sharp, and the minima in the cross sections at angles $\theta > 90^\circ$ are shifted somewhat toward smaller angles (the shift being different for different nuclei). The choice of the parameters d_r , d_i , V_{CI} , r_0 and δ could be made by the method described previously, in which one considers a series of fixed values of one of the parameters, for example V_{CI} . It turned out, however, that the value $V_{CI} = 11$ Mev, used by BF, enables us to find the range of values of the parameters d_r , d_i , r_0 and δ for which the cross sections σ_t and σ_r are in good agreement with experiment. We chose the following parameter values:

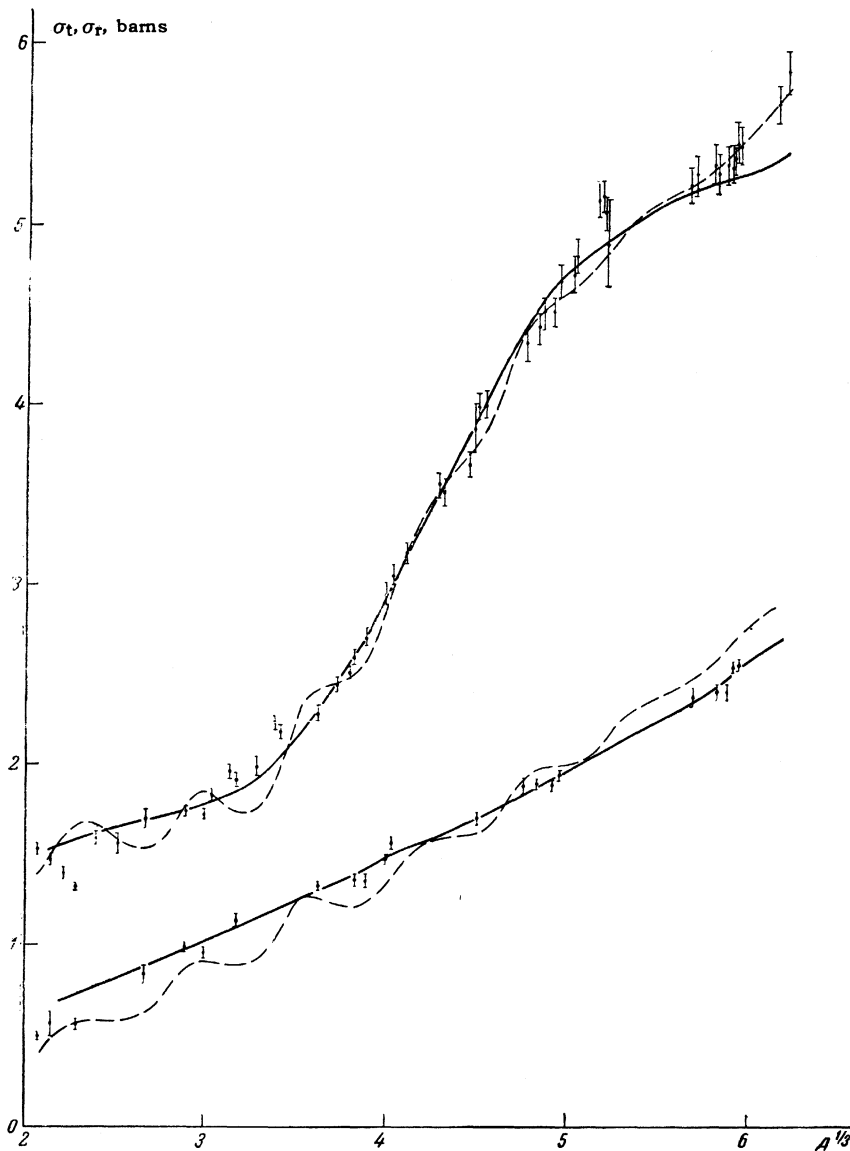


FIG. 2. Comparison of theoretical and experimental dependence of σ_t (upper curves) and σ_r (lower curves) on mass number A . The solid lines are the theoretical cross sections calculated for the potential (1) with the parameter values (3); the dashed lines are theoretical cross sections from [2]. The experimental data, indicated by the vertical dashes, are taken from [7, 8].

$$\begin{aligned}
 V_{CR} = 44 \text{ Mev}, & & V_{CI} = 11 \text{ Mev}, & & V_{SR} = 7.7 \text{ Mev}, \\
 d_r = 3.36 \text{ f}, & & d_i = 1.62 \text{ f}, & & r_0 = 1.25 \text{ f}, \\
 & & \delta = 0. & & (3)
 \end{aligned}$$

The cross sections σ_t and σ_r calculated with these parameter values are shown together with the experimental data in Fig. 2. For comparison we also give the analogous curves from [2]. The results demonstrate the considerable improvement in the agreement with experiment, especially for the light nuclei.

Although the choice of parameters was made on the basis of the integral cross sections, the agreement of the differential elastic cross section with experiment is good on the whole (Fig. 3). This is an additional confirmation of the correct choice of the parameters. The absence of deep minima and strong backward scattering in the computed angular

distributions shows that the defects cited in the introduction are eliminated by using the potential (1). The reduction of the cross section for elastic scattering at angles $\sim \pi$ is associated with the spin-orbit interaction (Fig. 4).* The introduction of surface absorption reduces considerably the oscillations in the diffraction pattern and makes possible a good description of the experimental integral cross sections for nuclei over almost the whole periodic table, with parameters which are independent of mass number A .

The agreement of the computed angular distributions with the experiments is not exact. But the optical model in its present form cannot pretend to give exact agreement, since it describes only the

*A qualitative explanation of this effect is given by I. S. Shapiro. [1]

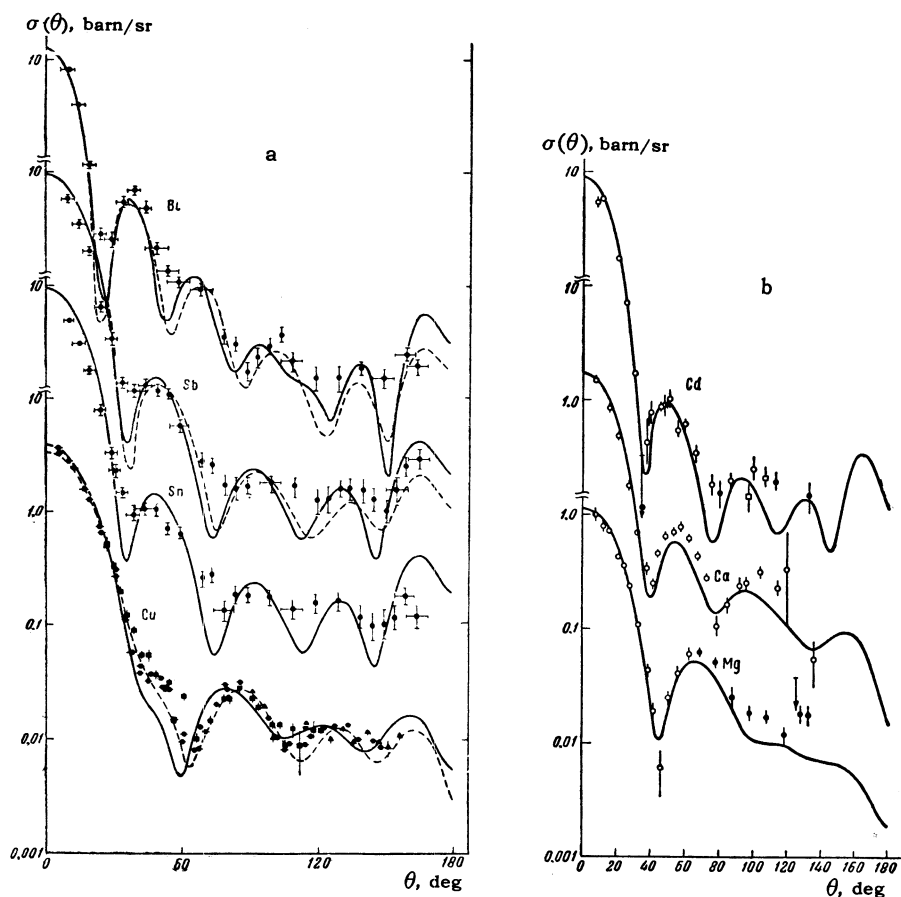


FIG. 3. Comparison of theoretical and experimental angular distributions of elastically scattered neutrons. The solid curves are the differential cross sections calculated with the potential (1) for the parameter values (3), for all nuclei except Mg, for which the computations were made with the potential (4) and the parameter $a = 0.74$ fermi, instead of $a = 0.65$ fermi (the value $a = 0.74$ fermi gives agreement with the experimental integral cross sections). The dashed curves are similar results from BF. The experimental data for Mg, Ca, Cd ($E_n = 14.6$ Mev) are taken from [9], those for Sn, Sb, Bi ($E_n = 14$ Mev) from [10], and those for Cu ($E_n = 14$ Mev) from BF. The computed values are for a neutron energy $E_n = 14$ Mev for all nuclei except Ca and Cd, for which $E_n = 14.6$ Mev (the difference in the results for $E_n = 14.6$ and 14 Mev being negligible). The ordinate scales for the various curves are shifted vertically.

averaged properties of nuclei. For example, it is known [12] that the differential cross section can change considerably from one isotope to another, i.e., for a change of A by one unit. At the same time, the optical model, in which the only dependence on A is via the nuclear radius ($R = 1.25 A^{1/3}$ fermi), can give only a smooth dependence on A and is incapable of explaining such variations.

Increasing V_{SR} from the Levintov value of 7.7 Mev to 10.35 Mev practically does not change the agreement with experiment (BF used the value $V_{SR} = 8.3$ Mev). This causes an essential reduction only in the backward elastic scattering, for which there are unfortunately no data. This dependence of the angular distributions on the spin-orbit coupling strength is demonstrated in Fig. 5, which shows the differential cross sections for different values of V_{SR} . Thus our preliminary

choice of the parameter V_{SR} is entirely reasonable, and could be improved only by using polarization data. It is interesting to note that the computed cross sections, including the differential cross sections, are practically unchanged when we reverse the sign of this parameter.

The insensitivity to the sign of the spin-orbit interaction is not difficult to understand. The spin-orbit terms which appear in the equations corresponding to the two values of the total angular momentum of the neutron ($j = l \pm 1/2$) differ only in having the factors l and $-(l + 1)$, respectively. For large l , we can neglect 1 compared to l . Consequently the amplitudes of scattered waves calculated from the solution of the equations with $j = l \pm 1/2$ will be close to those calculated for the equations with $j = l + 1/2$ in which we have changed the

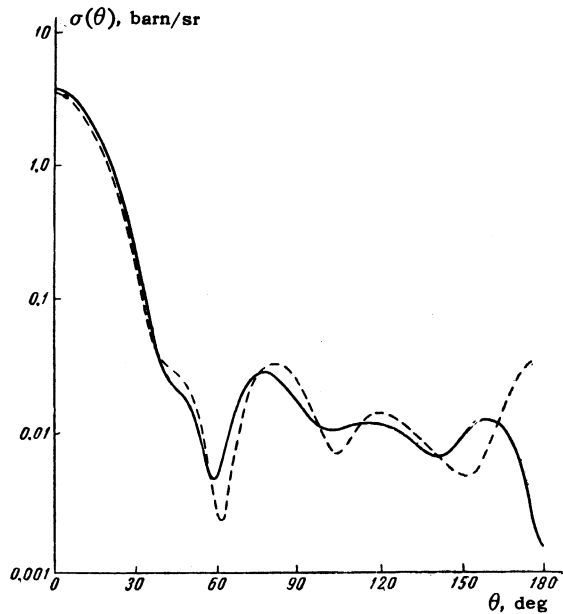


FIG. 4. Influence of spin-orbit interaction on differential elastic scattering cross section: solid curve for $V_{SR} = 8.28$ Mev, dashed curve for $V_{SR} = 0$.

sign of V_{SR} . For large l , the cross sections are symmetric under interchange of the amplitudes obtained from the equations corresponding to the two

different values of the total angular momentum of the neutron. Therefore the corresponding partial waves are insensitive to a change in sign of V_{SR} . For small l the change in sign of V_{SR} is unimportant because the spin-orbit potential is small compared to the other terms in the equation. Thus the insensitivity of the cross sections to the change in sign of V_{SR} is caused, on the one hand, by the smallness of the spin-orbit coupling, which in particular cases permits us to treat the spin-orbit term as a perturbation, and on the other hand by the smallness of the neutron spin compared to the orbital angular momentum when l is sufficiently large. For the same reasons, changing the polarization of the elastically scattered neutrons practically reduces to just a change in sign.

The picture is different when we consider bound states on the shell model, where the sign of the spin-orbit coupling constant is extremely important, since it determines the ordering of the levels with different values of j . As shown by experiment, the levels with $j = l + \frac{1}{2}$ always lie below those for $j = l - \frac{1}{2}$, i.e., the potential should be deeper for the first case. This determines the sign of the spin-orbit interaction in the shell model. The

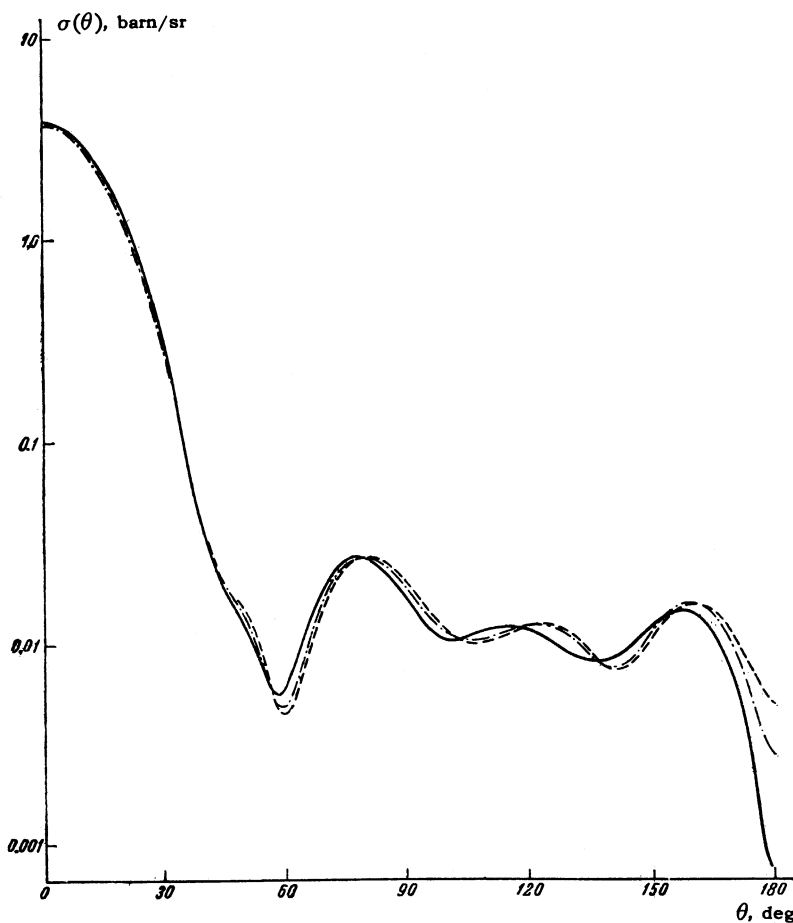


FIG. 5. Dependence of angular distribution on strength of spin-orbit coupling: solid curve for $V_{SR} = 10.35$ Mev, dot-dash curve for $V_{SR} = 8.3$ Mev, dashed curve for $V_{SR} = 7.7$ Mev.

computations in the present work were made with the sign which gives the correct ordering of levels.

3. THE WOODS-SAXON POTENTIAL AND ITS COMPARISON WITH THE POLYNOMIAL POTENTIAL

Except for the parameters d_r and V_{SR} , all the parameters of the potential (1), for which one can get a good description of the experimental cross sections, agree with those of BF. As was shown above, the difference in the values of the parameter V_{SR} (7.7 and 8.3 Mev) cannot be significant. But our value of d_r (3.36 fermi) gives a value of the diffuseness $\Delta \approx 3.44$ fermi which is considerably different from the value $\Delta \approx 2.84$ which follows from BF. (Δ is the size of the region over which the absolute value of the real part of the potential drops from 0.9 to 0.1 of its maximum value.) In order to find the reason for this disagreement, calculations were made with a potential having the same parameters as BF:

$$\rho(r) = \left[1 + \exp\left(\frac{r-R}{a}\right)\right]^{-1}, \quad q(r) = \exp\left[-\left(\frac{r-R}{b}\right)^2\right];$$

$$a = 0.65 \text{ f}, \quad b = 0.98 \text{ f}, \quad R = 1.25 A^{1/3} \text{ f},$$

$$V_{CR} = 44 \text{ Mev}, \quad V_{CI} = 11 \text{ Mev}, \quad V_{SR} = 8.3 \text{ Mev.}$$

(4)

Computations were done with the potential (4) for Al and Cu. In both cases the computed integral cross sections were lower than the experimental values and, consequently also lower than the theoretical cross sections of BF. The difference in the total cross sections reaches around $\sim 6-8\%$. The results are given together with the experimental data in Table I. In the same table we give the results of computations for Cu using a potential of the form (1), giving a least squares fit to potential (4) (so that the diffuseness is almost the same for both). The cross sections found for these two potentials differ relatively little; in particular the total cross sections differ by less than 2%. There is a somewhat larger difference between corresponding cross sections σ_r , apparently re-

sulting from the fact that the approximation of the Gaussian by a fourth-degree polynomial is not sufficiently accurate.

A comparison of the corresponding differential cross sections is shown in Fig. 6. In the region of large angles, the angular distribution for the polynomial potential is shifted somewhat to the left relative to the analogous curve for the potential (4). A comparison of the results for potentials (1) and (4), giving a least-squares fit to one another, shows that potentials with the same diffuseness give almost equivalent results, irrespective of the analytic form of the functions describing the potential.

In the computations with the potential (4), we again used the Runge-Kutta method for solving the Schrödinger equation. However in this case the solution at the initial point is not known analytically. We therefore found it by two different methods: either by representing the solution as a power series and determining the coefficients in the expansion from the condition that the solution be finite at the origin, or by choosing the starting point r_1 at some distance from the center of the nucleus, where the change in the potential can still be neglected and where, consequently, we can obtain a solution in analytic form. The computations of the starting data must be carried to the required accuracy. In particular, when the solution near the origin is represented in terms of spherical Bessel functions one should use the exact tables,^[13] since the use of the usual recursion relations leads to a great loss of accuracy. The exactness of the solution of the equation also is determined by the choice of step in the Runge-Kutta method and by the joining radius, beyond which the nuclear potential is set equal to zero. Our values for these quantities are in good agreement with those of Buck et al.^[14] Table II illustrates the dependence of the computational results on the position of the initial and final points, $x_1 = k_0 r_1$ and $x_2 = k_0 r_2$, for the case of Cu with a

Table I

	σ_t, b		σ_r, b	
	Al	Cu	Al	Cu
Experiment [7,8]	1.73±0.03	2.96±0.06	0.97±0.02	1.49±0.02
Theory, with potential and parameters (3)	1.77	2.96	1.01	1.49
Theory with potential (4)	1.63	2.73	0.97	1.40
Theory with potential (1) approximating potential (4)	—	2.69	—	1.33
According to BF [8]	—	—	1.02	1.50

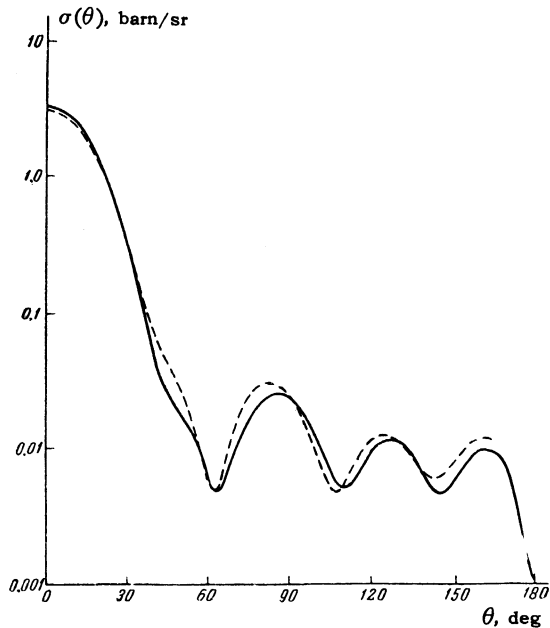


FIG. 6. Comparison of differential cross sections for Cu, calculated using potential (4) (solid curve), and with a potential (1) giving a least-squares fit to potential (4) (dashed curve).

particular choice of parameters ($k_0 = \sqrt{2MV_{CR}/\hbar^2}$). The results of the computation, using the two different methods for determining the starting values, agree to sufficient accuracy. We give them, in barns:

	σ_t	σ_s	σ_r
Expansion in power series:	2.732	1.329	1.403
Using solution for constant potential:	2.733	1.329	1.404

The correctness of the calculations with potential (1) was checked by a hand computation. The program for potential (4) was entirely analogous to that for potential (1). The only difference between the programs arose from the difference between the right hand sides of the equations, and the calculation of these was also checked by hand computation. Thus we may assume that our results are reliable.

4. CONCLUSIONS

1. Using a potential with surface absorption and including spin-orbit coupling, one can get a satisfactory description of the experimental cross sections (total, absorption and elastic) for a wide range of nuclei, with a set of parameters which is independent of mass number A .

2. One can equally well use a potential described by polynomials or a potential of the Woods-Saxon type, since to sufficiently good approximation they give equivalent results.

3. Our computations using the potential and parameter values given by Bjorklund and Fernbach^[3] give integral cross sections which are

Table II

x_1	x_2	σ_t, b	σ_s, b	σ_r, b
0.871	11.871	2.736	1.332	1.404
0.871	13.871	2.745	1.337	1.408
0.871	15.871	2.746	1.338	1.408
0.871	17.871	2.746	1.338	1.408
0.871	25.871	2.746	1.338	1.408
0.4355	20.4355	2.746	1.338	1.408
2.2451	20.2451	2.747	1.339	1.408
3.2451	20.2451	2.751	1.344	1.408
2.2451	11.2451	2.731	1.335	1.396

somewhat different from the results in their paper. In particular, the total cross sections calculated by us are less than the experimental values (with a difference which reaches $\sim 6-8\%$).

The authors express their sincere thanks to Prof. I. S. Shapiro for his interest in the work and discussion of the results; to Prof. A. N. Tikhonov, under whose direction the computational part of the work was done, and to V. M. Martynova, who did most of the programming and the computations on the "Strela" digital computer of Moscow State University.

¹ R. D. Woods and D. S. Saxon, Phys. Rev. **95**, 577 (1954).

² Luk'yanov, Orlov, and Turovtsev, JETP **35**, 750 (1958), Soviet Phys. JETP **8**, 521 (1959); Nuclear Phys. **8**, 325 (1958).

³ F. Bjorklund and S. Fernbach, Phys. Rev. **109**, 1295 (1958).

⁴ Culler, Fernbach, and Sherman, Phys. Rev. **101**, 1047 (1956).

⁵ Wyatt, Wills, and Green, Phys. Rev. **119**, 1031 (1960).

⁶ I. I. Levintov, JETP **30**, 987 (1956), Soviet Phys. JETP **3**, 796 (1956).

⁷ Coon, Graves, and Barschall, Phys. Rev. **88**, 562 (1952).

⁸ MacGregor, Ball, and Booth, Phys. Rev. **108**, 726 (1957).

⁹ W. G. Gross and R. G. Jarvis, Nuclear Phys. **15**, 155 (1960).

¹⁰ L. A. Rayburn, Phys. Rev. **116**, 1571 (1959).

¹¹ I. S. Shapiro, UFN **75**, 61 (1961), Soviet Phys.-Uspekhi **4**, 674 (1962).

¹² Vanetsyan, Klyucharev, and Fedchenko, Atomnaya Énergiya **6**, 661 (1959).

¹³ Tables of Spherical Bessel Functions, New York, 1947.

¹⁴ Buck, Maddison, and Hodgson, Phil. Mag. **5**, 1181 (1960).

Translated by M. Hamermesh